Photovoltaic Power Injection to the Grid with Reactive Power and Harmonic Compensation Using a Simple H Bridge Converter

Omar González, Javier Pérez-Ramírez, José A. Beristáin
Dpt. of Electrical and Electronics Engineering
Sonora Institute of Technology
Obregon City, Sonora, México
Email: omar.gonzalezsalazar.mx@ieee.org, javier.perezr@itson.edu.mx, jose.beristain@itson.edu.mx

Abstract— **This paper presents a study on the utilization of a single phase three-level bridge inverter to inject active power from a photovoltaic power source. Simultaneously, it compensates reactive power and harmonic current components, allowing power factor correction (PFC). An analysis on the design of passive elements, considering active and reactive power maximum values, is made. Additionally, the process of power injection is described in a straightforward way, whenever photovoltaic active power is available. Simulation results are presented to validate the design criteria, photovoltaic injection description, and PFC. A 5 kW - 10 kvar system is proposed a case of study. Simulations show that the three functions can be made without intervening with each other.**

Keywords—Active filter; bridge inverter; harmonic distortion; photovoltaic systems; power factor correction; power quality.

I. INTRODUCTION

Among the solutions for solving the current growing power consumption [1], two lines of research have emerged: the study of new power generation methods and the study of better energy consumption techniques. Concerning alternative power generation methods, most of the researchers have chosen renewable energies due to their availability: one of the most utilized is photovoltaic (PV) power generation. Countries such as the United States of America [2] and Germany [3] are world leaders on installed capacity and technology development. Latin-American countries, like Mexico [4], have an enormous PV potential because of its geographical and meteorological conditions. Nevertheless, generating more power is not enough for solving the energy deficiency problem; moreover, a significant improvement must be done in the way electricity is consumed. Contemporaneous loads have come with issues such as harmonic current consumption and low efficiency in the use of energy. Poor power quality is caused by linear and nonlinear loads connected to the mains [5]. In order to achieve better energy utilization, power quality in distribution systems has to be improved; several solutions have been proposed for the latter, among which, it is found: reactive power compensation and harmonic current compensation. These two types of compensation can be done either by passive components or by power electronic converters. Static Synchronous Compensator (STATCOM) and Active Power Filter (APF) are two well-known compensators based on power electronic converters [6], [7].

On the other hand, due to the nature of PV power generation, electronic power devices are required to convert dc voltage into ac voltage. There exist an abundance of topologies for power injection (see [8, 9] and the references therein). Several works [10-15] have taken advantage of these topologies in order to merge two functionalities into a single device, which allows active power injection and power quality improvement in a single converter.

Some of the used topologies are directly connected to the dc link; others have active elements working as dc-dc converters, in between. The systems proposed in [10] and [11] use a Boost converter to adequate dc link voltage; one of their main disadvantages is that the efficiency of the entire system reduces as the number of switching devices increases.

Other topologies based on three-phase systems, where the PV array is directly connected to the bridge, are described in the literature. Reference [12] provides a power analysis when such a device is utilized, but it does not explain the design criteria of passive elements, neither the process of active power injection. In [13] a cascaded control is used; it analyses the inverter, but the design of passive elements and power injection are not explained. An adaptive control scheme is presented in [14]: it uses a dq transformation for reference acquisition and focuses more in the control strategy than in the design process.

On the other hand, [15] considers a single phase grid-connected converter to inject PV energy and compensate reactive power altogether with harmonics. The control scheme used is a cascaded configuration, based on Static Reference Frame (SRF) transformations. Its drawbacks are that the sizing of passive elements is not explained and photovoltaic power injection consists only in the surplus power generated by the PV array.

Problem statement: From the discussion above and to the best of our knowledge, there is a lack of analysis on the sizing of passive elements in compensators, based on three-level bridge converters and renewable-power oriented. Moreover, PV power injection has not been properly described in previous works.

Contribution: A single-phase three-level bridge inverter, for power injection and power quality improvement, named

(for brevity) PV-compensator, is presented in this paper. This allows achieving PFC under a renewable power source scheme. In this work, it is considered the sizing criteria of passive elements. Explicit equations are presented to size elements for a given maximum active and reactive power capacity and a methodology is provided on how the power generated by PV means is taken from the dc side and transferred to the mains.

Organization: This paper is structured as follows. Next section introduces the device and gives a power analysis to determine model and design equations. Section III validates the design criteria through simulation results. In section IV conclusions are presented.

II. MODELING, DESIGN AND CONTROL

A. General description of the system

The complete schematic diagram of the proposed configuration is shown in Fig. 1.

A bridge inverter is constructed with four transistors (Q_1-Q_4), each of them with its own antiparallel diode (D_1-D_4). The power losses of the bridge are represented by the resistance R. A capacitor (C) is connected at the dc side of the inverter to keep a stabilized dc voltage (v_{dc}). The photovoltaic array is connected to the dc link; it provides a current (i_{PV}) when a voltage is set at its terminals.

The ac side voltage of the inverter (v_{inv}) is coupled to the grid voltage (v_g) through an inductance (L). The mains supply power to a set of loads that consume active, reactive and harmonic currents.

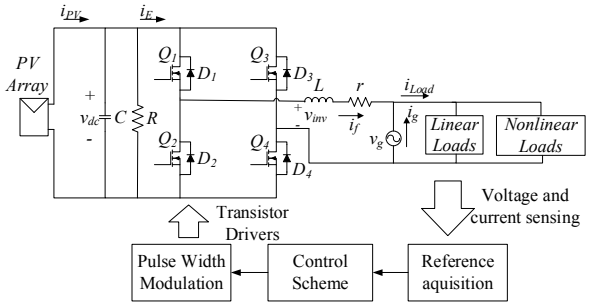

Fig. 1. Complete scheme of a PV-compensator.

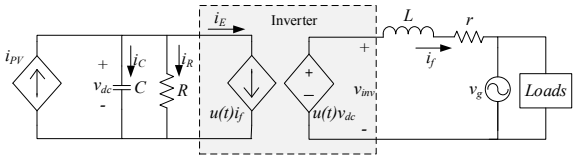

Fig. 2. Equivalent circuit for average model of PV-compensator.

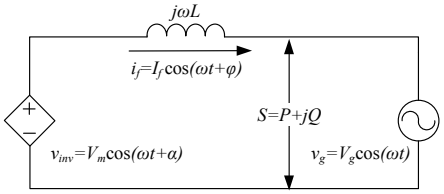

Fig. 3. Simplified circuit for the PV-compensator.

The injected current by the converter (i_f) and the currents required by the loads (i_{Load}) are sensed, then they are processed and introduced into a control scheme to achieve compensation. The resulting control signal ($u(t)$) is then fed into a Pulse Width Modulation (PWM) block that generates the correct switching sequence for the transistors.

B. Operation of the PV-compensator

1) Power flow analysis

The system operation is described based on the average model of a three-level inverter [16]. Fig. 2 shows an equivalent circuit using the average model. As detailed in [16], the average model of the inverter is given by

$$v_{inv} = u(t)v_{dc} \tag{1}$$

$$i_E = u(t)i_f \tag{2}$$

where $u(t)$ is the modulating or control signal.

To accomplish the model of the whole system, the passive elements and the PV array are added; thus, the mathematical model of the single phase PV-compensator is described as follows:

$$\frac{di_f}{dt} = \frac{1}{L}\left(-ri_f + u(t)v_{dc} - v_g\right) \tag{3}$$

$$\frac{dv_{dc}}{dt} = \frac{1}{C}\left(-u(t)i_f - \frac{1}{R}v_{dc} + i_{PV}\right) \tag{4}$$

For better understanding of the PV-compensator operation, a power flow analysis is carried out; in order to simplify it, series resistance (r) of L is neglected as shown in Fig. 3. The modulating signal for the inverter is given by

$$u(t) = m\cos(\omega t + \alpha)\,, \tag{5}$$

where ω is the angular frequency ($\omega=2\pi f$), α is the phase angle with respect to v_g, and m is the modulation index, $m \in [0,1]$. Therefore, the output voltage v_{inv} results:

$$v_{inv} = u(t)v_{dc} = V_m\cos(\omega t + \alpha) = mv_{dc}\cos(\omega t + \alpha)\,, \tag{6}$$

where V_m is the amplitude of v_{inv}. From Fig. 3, the complex power (S_L) is determined by (7). Equations (8) and (9) present active (P) and reactive (Q) power, respectively.

$$\begin{aligned} S = VI^* &= \frac{V_g I_f\cos(\varphi)}{2} - j\frac{V_g I_f\sin(\varphi)}{2} \\ &= \frac{V_m V_g}{2\omega L}\sin(\alpha) + j\left(\frac{V_m V_g}{2\omega L}\cos(\alpha) - \frac{V_g^{\,2}}{2\omega L}\right) \end{aligned} \tag{7}$$

$$P = \frac{V_m V_g}{2\omega L}\sin(\alpha) = \frac{V_g I_f\cos(\varphi)}{2} \tag{8}$$

$$Q = \frac{V_m V_p}{2\omega L}\cos(\alpha) - \frac{V_p^{\,2}}{2\omega L} = \frac{V_g I_f\sin(\varphi)}{2} \tag{9}$$

In (8) it is seen that the flow direction of active power only depends on α whereas the magnitude of P depends on V_m and

α. If α is negative, the inverter is consuming active power due to power losses in the transistors and maintaining a constant dc voltage level in the capacitor. On the other hand, if a power supply is connected into the dc link and α is positive, the result is active power (P) injected to the mains.

Equation (9) exposes the dependence of reactive power (Q) on V_m and α. The amount and direction of the reactive power is mostly determined by the amplitude of V_m. If V_m is greater than V_g, then the compensator works in capacitive mode. Otherwise, when V_m is inferior to V_g, it works in inductive mode.

2) Photovoltaic power injection

Considering the output voltage of the inverter as defined in (6), and dc link voltage regulated as a constant level, that is, $v_{dc}=V_{dc}$*, (8) can be rewritten as:

$$P = \frac{m v_{dc} V_g}{2\omega L}\sin(\alpha)\,. \tag{10}$$

A straightforward way to explain the photovoltaic power injection made by the compensator is to consider that i_{PV} is injected into the dc side of the converter. For that reason, some parameters must change in order to maintain the dc level regulated; it can be seen from (6) that m and α are the parameters that have to change in order to achieve this goal. On the other hand, from (10) it is seen that P also depends on m and α. This means that if active power is available in the dc side of the PV-compensator, m and α will be adjusted and power will be driven straight to the grid.

C. Passive component sizing

1) Inductance sizing

Solving for L in (8) we have

$$L = \frac{V_m V_g \sin(\alpha)}{2\omega P} \tag{11}$$

Substituting (11) in (9) and solving for α yields

$$\alpha = \arcsin\left(\frac{-PV_g}{V_m\sqrt{Q^2+P^2}}\right) - \arctan\left(\frac{-P}{Q}\right) \tag{12}$$

For the maximum reactive power, $m=1$, and for the same amount of reactive power compensation in capacitive and inductive mode $V_m=2V_g$. Therefore L can be calculated by:

$$L = \frac{V_g^2 \sin(\alpha)}{\omega P_{\max}} \tag{13}$$

where α is described in (12) with $P = P_{\max}$ and $Q = Q_{\max}$.

2) Capacitor sizing

Solving (4) for v_{dc}:

$$v_{dc} = \frac{mI_f}{4\omega C}\sin(2\omega t) + \tilde{V}_{dc}\,, \tag{14}$$

where I_f is the peak value of i_f.

From (14) it is seen that v_{dc} has two components: the dc voltage component (V_{dc}) and the peak to peak voltage ripple (Δv_{dc}) given by

$$\Delta v_{dc} = \frac{2mI_f}{4\omega C}\,. \tag{15}$$

From (8) and (9) we have that

$$I_f = \frac{2P}{V_g\cos(\varphi)} \tag{16}$$

$$I_f = \frac{2Q}{V_g\sin(\varphi)} \tag{17}$$

Since both (16) and (17) refer to the same variable, it follows that:

$$\frac{\sin(\varphi)}{\cos(\varphi)} = \tan(\varphi) = \frac{Q}{P} \Rightarrow \varphi = \arctan\left(\frac{Q}{P}\right) \tag{18}$$

Obtaining C from (15), there are two possible mathematical expressions for it, both in terms of the maximum active power ($P_{\max}$) and the maximum reactive power ($Q_{\max}$):

$$C = \frac{P_{\max}}{\omega\Delta v_{dc} V_g \cos\left(\arctan\left(\frac{Q_{\max}}{P_{\max}}\right)\right)} \tag{19}$$

$$C = \frac{\mathrm{Q}_{\max}}{\omega\Delta v_{dc} V_g \sin\left(\arctan\left(\frac{Q_{\max}}{P_{\max}}\right)\right)} \tag{20}$$

Both equations are equivalent and C can be calculated with either (19) or (20).

D. Reference acquirement and control

The PWM scheme employed in this work is shown in Fig. 4; it consists on a comparison between a triangular signal at a frequency f_s and a modulating signal $u(t)$, which is obtained from the cascaded control strategy shown in Fig. 5. An inner loop is used to regulate the injected current, i_f, while the outer loop is employed for dc voltage regulation. This is done by two Proportional-Integral (PI) controllers. Both have been tuned using a heuristic method. The inner loop must be faster than the outer one [14].

Some reference signals used by the control scheme are obtained via voltage and current sensors. This is the case of dc link voltage, v_{dc}, and injected current, i_f. However, i_h* and I_q* are acquired using single phase dq transformation of i_{Load}, as seen in Fig. 6. Signal i_q* is a reactive current reference that is in quadrature with v_g i.e. magnitude I_q* multiplied by $\sin(\omega t)$. The single phase dq transformation and its inverse are described by (21) and (22) respectively [17]:

$$\begin{bmatrix} i_d \\ i_q \end{bmatrix} = \begin{bmatrix} \cos(\omega t) & \sin(\omega t) \\ -\sin(\omega t) & \cos(\omega t) \end{bmatrix}\begin{bmatrix} i_{Load} \\ i_{Load+90^\circ} \end{bmatrix} \tag{21}$$

$$\begin{bmatrix} i_{Load} \\ i_{Load+90^\circ} \end{bmatrix} = \begin{bmatrix} \cos(\omega t) & -\sin(\omega t) \\ \sin(\omega t) & \cos(\omega t) \end{bmatrix} \begin{bmatrix} i_d \\ i_q \end{bmatrix} \quad (22)$$

The load current, i_{Load}, is introduced to a dq transformation. Signals in the Stationary Frame are composed by dc and ac components. The dc component corresponds to the fundamental frequency and the ac component contains all the harmonics of i_{Load}. By eliminating dc levels, harmonics are obtained in the dq frame. Applying the inverse transformation, harmonics are obtained in the time domain. Since for reactive current reference only the amplitude I_q* is needed, signal i_q is filtered from high frequencies and I_q* is given by the dc level.

III. Simulation Results

All simulations presented are obtained on PSIM® simulation software. Parameters for the employed circuits are presented in TABLE I.

1) Design validation

Using (13) and (19) L and C have been calculated for 5 kW (P_{max}) and 10 kvar (Q_{max}). Fig. 7 shows the circuit used for simulations. This simulation corroborates that the designed passive elements can manage the maximum power ratings.

Active and reactive powers injected to the grid are shown in Fig. 8(a). Simulation was set to extract the power magnitudes for which C and L were designed. It is shown that after a transient time, steady state values go to 5 kW and 10 kvar. This determines that the system has the capability to manage the maximum ratings for which it was sized.

Fig. 8 (b) shows the dc link voltage. Control strategy can regulate it at 360 V and the associated ripple stays around 10 % of it (37 V).

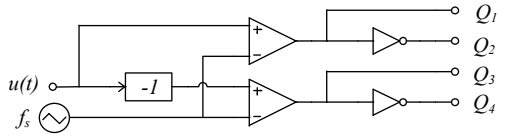

Fig. 4. Schematic representation of PWM.

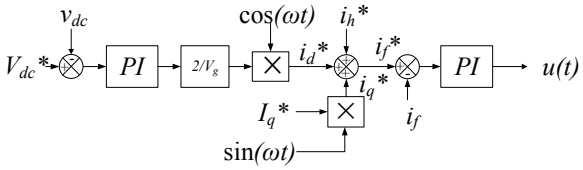

Fig. 5. Cascaded control scheme used for PV-compensator.

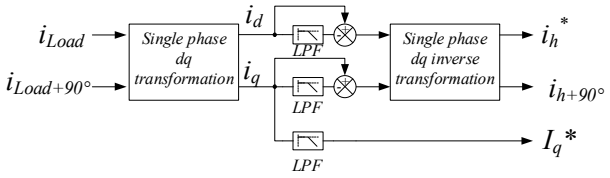

Fig. 6. Acquirement of harmonic and reactive current references.

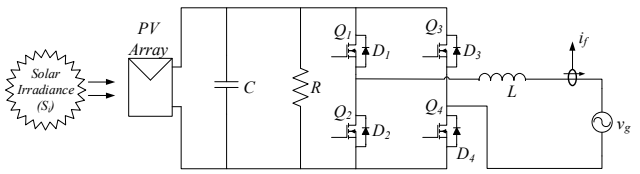

Fig. 7. Simulation circuit for the validation of photovoltaic power injection.

TABLE I. Parameters for Simulation Circuits

Simulation Parameters			
Parameter	**Value**	**Parameter**	**Value**
V_g	180 V	C_B	1 mF
V_{dc}*	360 V	L_S	400 µH
ω	120π rad/s	S_i	1000 W/m^2
Δv_{dc}	10% of V_{dc}*	P_{ac}	1 kW
L	4.1 mH	P_{dc}	1 kW
C	4 576 µF	Q_L	3 kvar
f_s	9600 Hz	*PV capacity*	5 kW$_{max}$ at 1000 W/m^2
R	500 Ω		

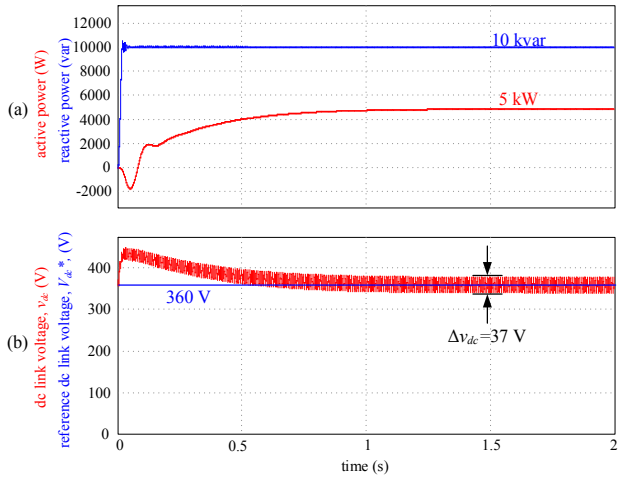

Fig. 8. Simulation results for design validation: (a) active and reactive power supplied, (b) dc link voltage and dc link voltage reference.

2) Photovoltaic power injection results

Fig. 9 (a) shows a simulation graphic of the active power injected for different values of solar irradiation, S_i; as it increases (decreases), so it does the active power injected to the mains. When irradiation is near to zero, the compensator takes the necessary real power from the grid to keep the capacitor charged; thus, the dc link voltage is regulated as shown in Fig. 9 (b).

3) Power quality improvement

Power quality improvement is another functionality of this converter. To prove this, a simulation is performed using the circuit shown in Fig. 10. The complete simulation graphics of the active and reactive power are shown in Fig. 11 (a); on the other hand, the dc link voltage is displayed in Fig. 11 (b). Three stages are identified with rectangles; each of them is inspected in detail in Fig. 12 to Fig. 15.

This simulation assumes the photovoltaic array is working at its maximum capacity. Three kinds of loads are connected to

the mains, consecutively: first, a resistive load (P_{ac}) is directly connected to the mains; second, an inductive load (Q_L) is shunt connected; then, a nonlinear load is added: it is constituted by a single phase bridge rectifier connected through a series inductance (L_S) that supplies power for a resistive load (P_{dc}).

Fig. 12 shows the simulation results of the first stage; it consists of a resistive load connected to the mains. Fig. 12 (a) shows the voltage v_g and the current i_g of the grid; both signals have the same phase, since only active power is consumed; the power factor (PF) is unitary. Fig. 12 (b) and Fig. 12 (c) show the power consumption of the load and the compensator,

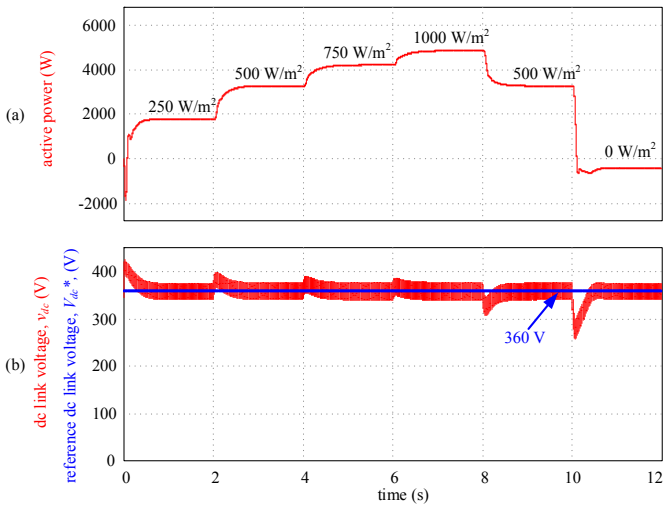

Fig. 9. Simulation of photovoltaic power injection: (a) active power, (b) dc link voltage and dc link voltage reference.

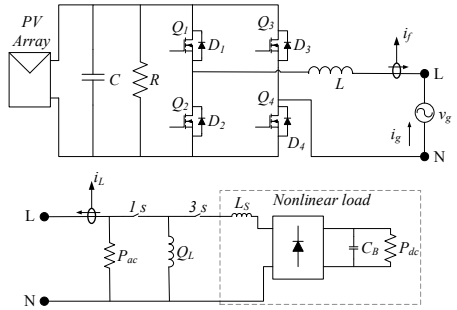

Fig. 10. Circuit for power quality improvement simulation.

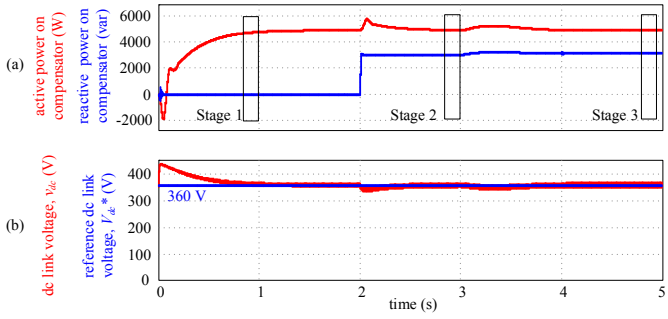

Fig. 11. Complete simulation: (a) active and reactive powers, (b) dc link voltage and dc link voltage reference.

respectively. The load is only using active power, while the compensator is only injecting the active power available on its dc side. Fig. 12 (d) shows a comparison between *u(t)* and v_g (scaled for better appreciation). Signal *u(t)* has a positive phase with respect to v_g, which is expected since it is necessary to transfer the active power generated by the photovoltaic array.

The simulation results corresponding to the second stage are shown in Fig. 13; it has been performed with active and reactive loads at fundamental frequency. In Fig. 13 (a) it is shown that i_g is delayed from v_g (PF=0.7897) before the compensation. After the compensation, PF rises to 0.999 and i_g is in phase with the grid voltage. This is because the compensator is dealing with the reactive power needed by the load: this can be contrasted in Fig. 13 (b) (load) and Fig. 13 (c) (compensator). Fig. 13 (d) displays *u(t)* and the normalized signal of grid voltage; it is seen that when reactive power is compensated, the amplitude of *u(t)* increments because the compensator operates in capacitive mode in order to compensate the inductive load.

The third stage of the simulation includes the compensation of harmonic currents; it includes all the functionalities of the PV-compensator, which demonstrates that they are independent. Fig. 14 shows the simulation results. In Fig. 14 (a) v_g and i_g are displayed. Before compensation PF is 0.937 and total harmonic distortion (THD) of the current is 37.374%. Once the harmonic current compensation function is activated, the current distortion is reduced to THD=3.771% and the PF rises to 0.999. At Fig. 14 (b), the current consumed by the load, i_{Load}, and the current provided by the converter, i_f, are shown. The harmonics required by the nonlinear load and the reactive power for the reactive load are provided by the compensator, whereas the real power generated in the photovoltaic array is injected to the mains; see Fig. 14 (c). Fig. 14 (d) shows *u(t)*, which has changed its waveform in order to supply a voltage such that i_f contains the harmonic components necessary to compensate i_{Load}. Fig. 15 (a) and Fig. 15 (b) show the frequency spectrum of the i_g and i_{Load} signals, previously exhibited in Fig. 14 (b), respectively.

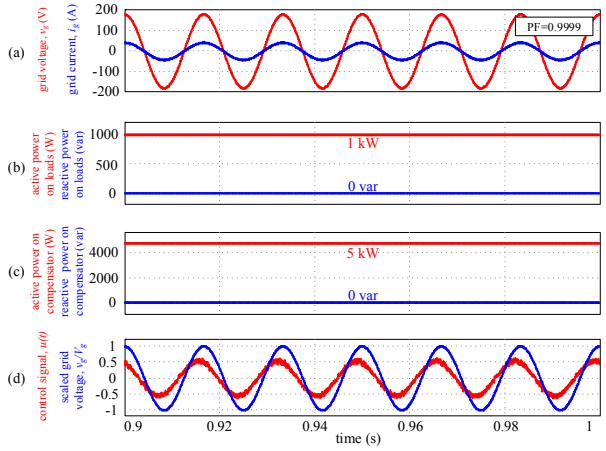

Fig. 12. Photovoltaic injection stage: (a) voltage and current of the grid, (b) active and reactive powers consumed by the load, (c) active and reactive powers of the converter, (d) control signal and voltage reference.

IV. CONCLUSIONS

A single three-level converter used as (a) an active power injector, (b) a reactive power compensator, and (c) a current harmonic compensator, was presented. Additionally, a methodology has been developed for designing of passive components, and a simple analysis for explaining the active power injection from a photovoltaic power generator has been provided. The proposed approach has been validated through simulations showing that the three aforementioned functionalities can be carried out at the same time without affecting each other.

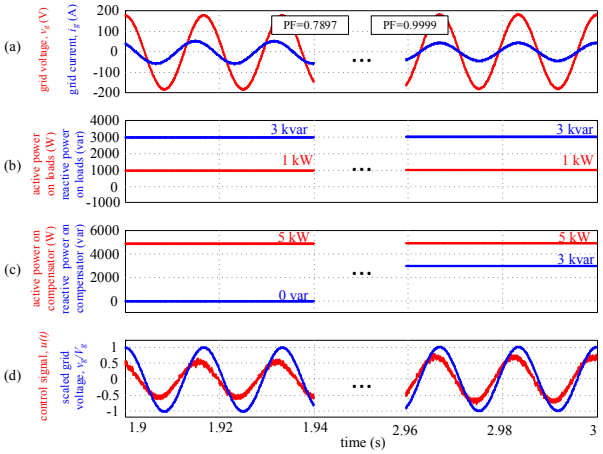

Fig. 13. Reactive power compensation stage: (a) voltage and current of the grid, (b) active and reactive powers consumed by the load, (c) active and reactive powers of the converter, (d) control signal and voltage reference.

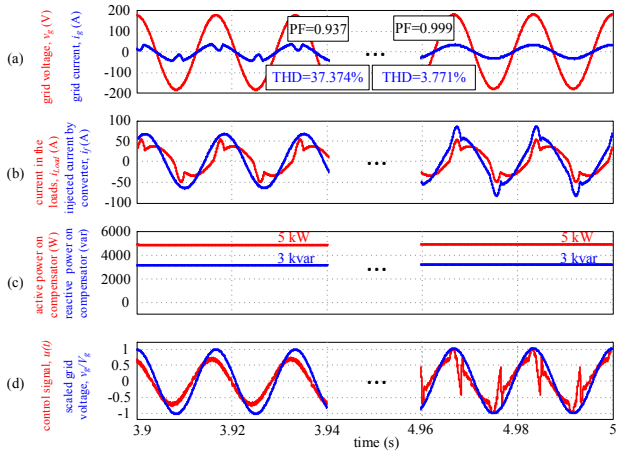

Fig. 14. Harmonic currents compensation stage: (a) voltage and current of the grid, (b) load current and converter current, (c)active and reactive powers of the converter, (d) control signal and voltage reference.

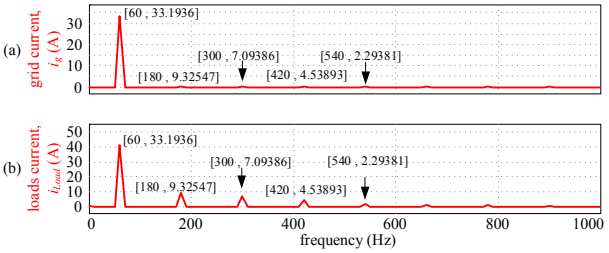

Fig. 15. Frequency spectrum of: (a) grid current, i_g , (b) load current, i_{Load}.

REFERENCES

[1] Kukreja, Rinkesh. 2014. "Causes And Solutions To The Global Energy Crisis - Conserve Energy Future". *Conserve-Energy-Future*. http://www.conserve-energy-future.com/causes-and-solutions-to-the-global-energy-crisis.php [Accessed: 2-Mar-2015]

[2] Solar Energy Industries Association, "Q3 2014 U.S. solar market insight report overview", 2014. [Online]. Available: http://www.seia.org/events/q3-2014-us-solar-market-insight-report-overview [Accessed: 25-Feb-2015].

[3] Fraunhofer, "Recent facts about photovoltaics in Germany", 2015. [Online]. Available: http://www.ise.fraunhofer.de/en/publications/veroeffentlichungen-pdf-dateien-en/studien-und-konzeptpapiere/recent-facts-about-photovoltaics-in-germany.pdf [Accessed: 15-Feb-2015].

[4] Mexican Secretary of Energy, "National renewable energies inventory", 2015. [Online]. Available: http://inere.energia.gob.mx/publica/version3.1 [Accessed: 25- Feb- 2015].

[5] S. Bhattacharyya and S. Cobben, "Consequences of poor power quality – An overview", *in Power Quality*, 1st ed., A. Eberhard, Ed. InTech, 2011, pp. 3-23.

[6] El-Habrouk, M.; Darwish, M.K.; Mehta, P., "A survey of active filters and reactive power compensation techniques," *Power Electronics and Variable Speed Drives, 2000. Eighth International Conference on (IEE Conf. Publ. No. 475)* , vol., no., pp.7,12, 2000.

[7] Akagi, H., "The state-of-the-art of active filters for power conditioning," *Power Electronics and Applications, 2005 European Conference on*, vol., no., pp.15 pp.,P.15, 0-0 0.

[8] Jedtberg, H.; Pigazo, A.; Liserre, M., "Robustness evaluation of transformerless PV inverter topologies," *Control and Modeling for Power Electronics (COMPEL), 2014 IEEE 15th Workshop on* , vol., no., pp.1,5, 22-25 June 2014.

[9] Saridakis, S.; Koutroulis, E.; Blaabjerg, F., "Optimal Design of Modern Transformerless PV Inverter Topologies," *Energy Conversion, IEEE Transactions on*, vol.28, no.2, pp.394, 404, June 2013.

[10] De Souza, K.C.A.; dos Santos, W.M.; Martins, D.C., "A single-phase active power filter based in a two stages grid-connected PV system," *Industrial Electronics, 2009. IECON '09. 35th Annual Conference of IEEE*, vol., no., pp.114,119, 3-5 Nov. 2009.

[11] Noroozian, Reza, and Gevorg B. Gharehpetian. "An investigation on combined operation of active power filter with photovoltaic arrays." *International Journal of Electrical Power & Energy Systems,* vol. 46, pp. 392-399, 2013.

[12] Varma, R.K.; Das, B.; Axente, I.; Vanderheide, T., "Optimal 24-hr utilization of a PV solar system as STATCOM (PV-STATCOM) in a distribution network," *Power and Energy Society General Meeting, 2011 IEEE* , vol., no., pp.1,8, 24-29 July 2011.

[13] Haoran Bai; Shuqi Shang, "A research of combined multifunctional three phase grid-connected inverter/active power filter for PV system," *Power Electronics for Distributed Generation Systems (PEDG), 2010 2nd IEEE International Symposium on* , vol., no., pp.224,228, 16-18 June 2010.

[14] Sant, A.V.; Khadkikar, V.; Weidong Xiao; Zeineldin, H.; Al-Hinai, A., "Adaptive control of grid connected photovoltaic inverter for maximum VA utilization," *Industrial Electronics Society, IECON 2013 - 39th Annual Conference of the IEEE* , vol., no., pp.388,393, 10-13 Nov. 2013.

[15] Campanhol, L.B.G.; da Silva, S.A.O.; Sampaio, L.P.; Junior, A.A.O., "A grid-connected photovoltaic power system with active power injection, reactive power compensation and harmonic filtering," *Power Electronics Conference (COBEP), 2013 Brazilian* , vol., no., pp.642,649, 27-31 Oct. 2013.

[16] González, O., "Design and implementation of an Active Power Filter", Bachelor of Science, Sonora Institute of Technology, pp. 21, 2014. (In Spanish).

[17] Gonzalez, M.; Cárdenas, V.; Pazos, F., "DQ transformation development for single-phase systems to compensate harmonic distortion and reactive power," *Power Electronics Congress, 2004. CIEP 2004. 9th IEEE International* , vol., no., pp.177,182, 17-22 Oct. 2004.